Semiconductor Nanoparticles in Photocatalysis: Emerging Art and Perspectives

A Sharma[1], A. Sharma[2], R. Sharma[3]
[1]Department of Electrical and Electronics Engineering, AKG College of Engineering, UP Technical University, NH-24 Bypass, Ghaziabad, Uttar Pradesh, India
[2]Department of Electrical Engineering, MP A&T University, Udaipur, Rajasthan, India
[3]Florida State University and Innovations And Solutions Inc.,3945 W Pensacola Street, Tallahassee, FL 32304
[1]Adhar Sharma: Paper is an undergraduate BE Electrical Engineering project

ABSTRACT

A principle of semiconductor nanophotocatalysis – a new trend in photochemistry deals with the photocatalytic redox-reactions with the participation of semiconductor nanoparticles. The origin of various size-dependent explanations in the semiconductor photocatalysis are spot light with the special attention paid to the quantum size effects originating from a spatial confinement of the photogenerated charge carriers (excitons) in ultra-small semiconductor nanoparticles (quantum dots). Our focus was the specifics of quantum-confined semiconductor nanoparticles including the size-dependent optical properties (the position and shape of absorption and photoluminescence bands, the oscillator strength of interband electron transitions, etc.), thermodynamic characteristics (the band gap, the potentials of conduction and valence band edges, the nature, number and depth of charge trapping sites, etc.), as well as the dynamics of photogenerated charge carriers (charge migration in semi-conductor nanoparticles, its localization on the structure defects, interfacial charge transfer, etc.). The consequences of spatial confinement were characterized in semiconductor nanoparticles affecting their photocatalytic behavior. The development of the photocatalytic properties in narrow-band-gap semiconductors at the nanoscale increased a number of photocatalytic reactions for a given nanocrystalline semiconductor as compared with the bulk material. The acceleration of photocatalytic reactions enhanced with the participation of semiconductor nanoparticles due to their size-dependent growth of the energy in charge carriers. The photoinduced polarization caused by the accumulation of excessive charge by semiconductor nanoparticles resulted an increase of their photocatalytic activity. The specific features of the photocatalytic behavior of semiconductor nanoparticles were size-related phenomena in the photocatalytic metal reduction, photocatalytic formation of binary semiconductor nanoheterostructures, photoinduced polymerization of acrylic monomers, photocatalytic reduction of sulfur compounds, and photocatalytic water reduction with the participation of semiconductor nanoparticles. The photochemical behavior of quantum-confined semiconductor nanoparticles was observed under powerful pulse illumination. The simultaneous and additive influences of different size effects showed dependence upon the photocatalytic properties of semiconductor nanoparticles. In conclusion, perspectives of future development of the photocatalytic systems based on nanostructured semiconductors broaden the number of nanophotocatalysts and photocatalytic processes, as well as the benefits of the utilization of such systems in modern nanotechnology.
Keywords: semiconductor, nanoparticles, photocatalysis, quantum dots

1 INTRODUCTION

Semiconductor nanoparticles (NPs) show remarkable thermodynamic, photophysical, photochemical, magnetic and dimensional organization other properties. Size Effects in Semiconductor Nanocrystals originate from surface area and layers. Quantum size effects are caused by changes in the electronic properties of semiconductor nanocrystals in the range of 1 nm (CuCl) to 100 nm (PbSe). Photonics of semiconductor NPs is new research on quantum size effects as changes in the electronic structure of semiconductor crystals in the range of R < aB. The phase size effect makes them stable to high-temperature or uncharacteristic phases.

2 SIZE EFFECTS OF SEMICONDUCTOR NPS

2.1 Surface Trapping and Interfacial Transfer of Charge Carriers: During this process, electron trapping in TiO2 NPs generates Ti3+ cations giving rise to the characteristic EPR signals and absorption bands at 600-900 nm. In the presence of oxygen, the conduction band electron can be captured in the form of anion-radical O^{2-} The trapped hole exists in TiO2 NPs as the radical $OH^{\bullet}$ or anion-radical O^{-} clearly visible in EPR spectra, and transient absorption spectra as a band centered at 450-460 nm. In metal-sulfide semiconductor NPs the hole trapping gives the anion-radicals S^{-}. Semiconductor NPs lack of band bending near the semiconductor solution boundary.

The charge carrier dynamics in semiconductor NPs affects directly the secondary redox processes: in the secondary "dark" chemical reactions participate trapped electrons and holes, rather than free charge carriers; the electron-hole recombination is suppressed considerably as compared with microcrystalline semiconductors; the rate of interfacial charge transfer is much higher in case of nanocrystalline semiconductors because of lack of the band bending on the semiconductor-solution interface boundary. Nanometer crystals of $Sr_2Ta_2O_7$ and $SrSnO_3$ are more active in the photocatalysis. The photocatalytic activity in iodide oxidation and the photocatalyst dispersion were found for many oxide semiconductors (ZrO_2, MoO_3, Fe_2O_3, ZnO, CeO2). The reduction of TiO_2 NP size from 300 to 20 nm is accompanied by 50% growth of the quantum yield of electron transfer from a RuII tris-bipyridyl complex

resulting from of an increase in the density of surface states capable of electron. The maximal quantum yield of the photocatalytic oxidation can be achieved for 10-15 nm TiO_2 particles. Different schemes explain the photoinduced electron transfer in following schemes.

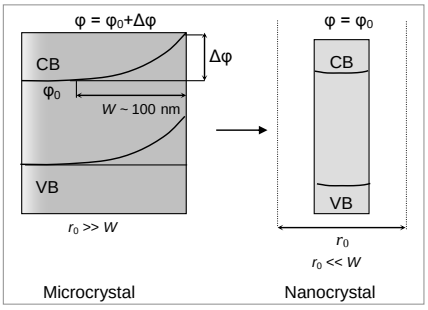

Scheme 1. Electric potential change on the semiconductor-solution boundary for semiconductor micro- and nanocrystals.

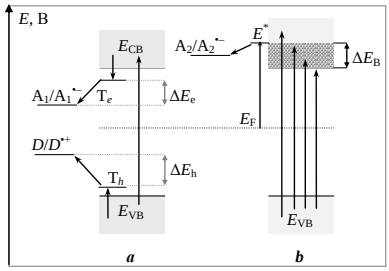

Scheme 2. Energy diagram of photocatalytic systems based on non-charged semiconductor NPs (case a) and the NPs in the state of photoinduced polarization (case b).

2.2 Semiconductor NC size and Photocatalytic activity: The semiconductor photocatalysts have large band gap (E_g > 2.2 eV). Size-dependent band gap expansion is helpful in development of photocatalytic properties in nanocrystals of semiconductors.The rate constant of the photoinduced electron transfer from CdS NPs is related with MV^{2+} and the size of semiconductor NPs as:

$$\lg(k/k^{bulk}) = -\alpha\Delta E = -\alpha(E_{CB}(R) - E^0(MV^{2+}/MV^{\bullet+}))$$

where k^{bulk} is the charge transfer rate constant for bulk CdS, α is a constant. A combined effect of the size-dependent band edge potential growth and the photoinduced polarization of semiconductor NPs determines the photocatalytic behavior of NPs as semiconductor Nanoheterostructures with Advanced Photocatalytic Properties

The quantum yields of semiconductor-mediated photocatalytic reactions are 0.1-0.2 due to loss of photogenerated charge carriers in various recombination processes. So, maximal quantum yield of photocatalytic processes may not be expected to be higher than 0.1.

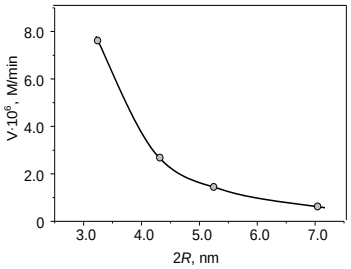

Fig 1. The relationship between the rate of photocatalytic Zn^{II} reduction and the size of ZnS NPs (2R). [ZnS] = 1×10^{-3} M, [Na_2SO_3] = 1×10^{-2} M, [$ZnCl_2$] = 2×10^{-3} M, pH 9.8

How to increase the efficiency of the photocatalytic systems based on the nanocrystalline semiconductor photoelectrochemical systems?.

Main choices are efficient spatial separation of charge carriers, minimization of the recombination losses in semiconductor NPs, and suppression of the secondary reverse reactions.

(i) coupled semiconductor nanostructures with concerted band energies, (ii) metal-semiconductor nanocomposites, and (iii) coupled nanostructures comprising a semiconductor and a conjugated polymer. The photocatalytic systems is based on mesoporous semiconductors and semiconductor NPs of anisotropic shape.

Charge separation in coupled semiconductor nanostructures: A combination of two nanocrystalline semiconductors differing in the band structure can favor conditions of the photogenerated electron separation and hole on different parts of the nanocomposite. Scheme 3 illustrates the charge separation in a coupled CdS/TiO_2 nanostructure.

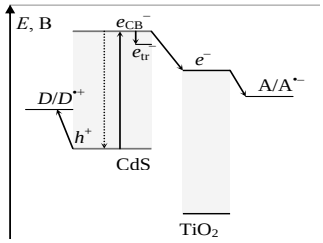

Scheme 3. Charge separation in a coupled CdS/TiO_2 nanostructure.

Photoexcitation of the CdS/TiO_2 nanostructures: It goes in one-way electron transfer from the conduction band of CdS NPs to TiO_2 NPs. Many coupled semiconductor nanostructures with advanced photocatalytic and photoelectrochemical properties are in use – CdS/TiO_2, $CdSe/TiO_2$, ZnS/TiO_2, PbS/TiO_2, Bi_2S_3/TiO_2, CdS/M_xS_y (M_xS_y = Bi_2S_3, Sb_2S_3, Cu_xS, Ag_2S), CdS/ZnO, CdS/AgJ, CdS/ZnS, ZnO/TiO_2, Cu_2O/TiO_2, ZnO/SnO_2, SnO_2/TiO_2, WO_3/TiO_2, WO_3/ZnO, MnO_x/TiO_2, In_2O_3/TiO_2, CeO_2/TiO_2, Fe_2O_3/TiO_2, ZrO_2/TiO_2, Cu_2O/ZnO, InP/TiO_2, $AgBr/TiO_2$, MoS_2/TiO_2, WS_2/TiO_2, $CdTe/TiO_2$, etc.

Generally, the charge separation rate in coupled semiconductor nanostructures is very high. For example, the rate constants of photoinduced electron transfer from CdS (CdSe) NPs to ZnO or TiO_2 NPs in the coupled CdS/ZnO, CdS/TiO_2 and CdSe/TiO_2 nanostructures are as high as 10^{10}-10^{12} s^{-1}. The electron transfer act occurs in 10-100 ps after the photoexcitation and can be as efficient as 100%, competing with the surface trapping and recombination of charge carriers.

The increased efficiency of primary charge separation results in growth of the quantum yields of photocatalytic reactions mediated by the coupled semiconductor nanostructures. For example, the said charge separation in the CdS/TiO_2 nanostructures is accompanied by acceleration of the oxidative photocorrosion of CdS NPs and Cd^{II} reduction on the surface of TiO_2 NPs. The coupled CdS/TiO_2 nanostructures show advanced photocatalytic properties in methylviologen reduction, oxidation of organic dyes, trichloroethylene and dimethylsulfide, dehalogenation of tetrachlorobenzene and hydrogen evolution from solutions of sacrificial donors. The CdSe/TiO_2 and Bi_2O_3/TiO_2, In_2O_3/TiO_2 and ZrO_2/TiO_2 nanostructures toward oxidation much higher. The α-Fe_2O_3/TiO_2 nanostructures act as an efficient photocatalyst of nitrate anion reduction with simultaneous sucrose oxidation.

Nanocomposites MS/Fe_3O_4 (M = Zn, Cd, Pb, etc.) and $Ag/TiO_2/SiO_2/Fe_3O_4$ show photocatalytic properties in solutions. Examples of narrow-band-gap semiconductor are CdS/TiO_2 and CdS/ZnO, CdSe/TiO_2, CdS_xSe_{1-x}/TiO_2, CdTe/TiO_2, Bi_2S_3/TiO_2, PbS/TiO_2, WS_2/TiO_2, Cu_2O/TiO_2, InAs/TiO_2, and CdTe/ZnO nanostructures showing quantum size effects of CdS NPs (E_{CB}-E_{VB}) levels(photocatalytic activity of Na_2S/Na_2SO_3 solution).

3 CdS, ZnO, TiO_2, SnO_2 NANOCOMPOSITES: AN EXCITING ART

Photoinduced charge transfer in the coupled nanostructured nanocomposites of polymers with TiO_2, ZnO and CdSe, can act as sensitizer of wide-band-gap semiconductor NPs and the hole-transporting layer and show high efficiency of the charge separation as well as the photocatalytic and photoelectrochemical activity.

The efficiency of photocatalytic reactions with the participation of nanocrystalline titanium dioxide can be substantially increased by combining TiO_2 NPs with nanostructured carbon materials – nanotubes, graphite, fullerenes, etc. For example, the nanocomposites of TiO_2 NPs with multi-wall carbon nanotubes show higher photocatalytic activity in oxidation of dyes. The *photocatalytic synthesis* of coupled semiconductor nanostructures, coupled TiO_2/MoS_2 and TiO_2/WS_2 nanostructures can be prepared by the photocatalytic decomposition of $(NH_4)_2MoS_4$ and $(NH_4)_2WS_4$, respectively, TiO_2/MoS_2 and TiO_2/WS_2 NPs show high photocatalytic activity toward oxidation. The photocatalytic reduction of sulfur with the participation of ZnO NPs and nanocrystalline TiO_2 films produces coupled ZnO/MS and TiO_2/MS nanostructures (where MS = CdS, PbS, CuS).

Colloidal ZnO nanorods 100-350 nm in length and 20-150 nm in the inner diameter can be produced by the ultrasound treatment of bulk ZnO powder. The relative positions of the potentials of conduction and valence band edges of CdS, ZnO and TiO_2 is favorable for the fast and irreversible spatial charge separation in ZnO/CdS and TiO_2/CdS nanostructures forming in photocatalytic reaction (Scheme 4).

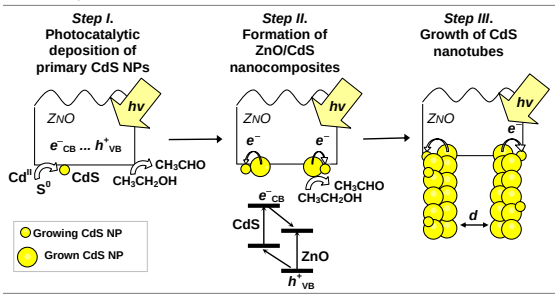

Scheme. 4. Photocatalytic formation of CdS nanotubes on the tips of ZnO nanorods.

The secondary reactions with spatially isolated electrons and holes, resulting in CdS deposition and formation of nanotubes (in case of ZnO) or nanorods (in case of TiO_2 films), occur apparently on the interface boundary between the metal-oxide and growing CdS NPs.

Photocatalytic processes with the participation of coupled semiconductor-metal nanostructures. The rate of photocatalytic reduction is limited by efficiency of the interfacial electron transfer from the surface traps of semiconductor NPs to electron acceptors. Semiconductor photocatalyst NPs coupled with metal NPs enhance efficinecy. The metal-semiconductor nanostructures are synthesized by mixing semiconductor and metal NPs on the surface of nanocrystalline semiconductor. Scheme 7 illustrates the energy level structure of metal-semiconductor nanocomposite along with the changes induced by the photoinduced polarization. The semiconductor and metal NPs being got into contact, a collective Fermi level establishes instantly (E_F^3 on Scheme 5) in the gap between the Fermi levels of the starting NPs (E_F^1 and E_F^2).

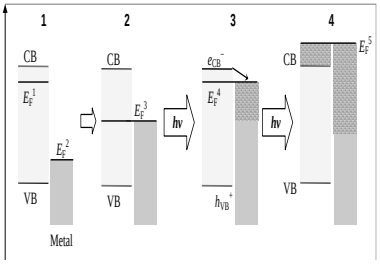

Scheme 5. Energy level structure of a metal-semiconductor nanocomposite.

The photoexcitation of composite NPs is accompanied by the interfacial transfer of electrons from the conduction band of the semiconductor to metal NPs resulting in an increase of the collective Fermi level (E_F[4]). Metal-semiconductor NPs TiO_2/Pt, TiO_2/Pd, TiO_2/Rh, TiO_2/Au, TiO_2/Ag, TiO_2/Cu, ZnO/Pd, ZnO/Ag, ZnO/Au, CdS/Pt, CdS/Au, and Fe_2O_3/Au show acceleration of the photocatalytic reactions. For example, deposition of Ag NPs onto the surface of nanocrystalline TiO_2 enhances the photocatalytic activity. The binary TiO_2/Au nanostructures show high photocatalytic activity. Deposition of Rh NPs onto the surface of nanocrystalline TiO_2 enhances the photocatalytic activity of the semiconductor in benzene oxidation. The coupled ZnO/Ag NPs have high photocatalytic activity in dyes destruction.

The quantum yield of photocatalytic hydrogen production from aqueous solutions is close to zero. Acceleration of the photocatalytic hydrogen evolution was observed for CdS/Pt, CdS/Rh, CdS/Ni, $ZnIn_2S_4$/Pt, TiO_2/Pt, TiO_2/Au, TiO_2/Ni, TiO_2/Cu, and TiO_2/Ag nanostructures. The coupled ZnO/Ag NPs are more active in the photocatalytic reduction of copper(II).

The phenomena discussed are most probably associated with *the size effects in metal NPs*. The growth of the size of a metal NP is accompanied with the growth of its capacity, which, in turn, dictates the efficiency of the charge transfer from a neighboring semiconductor NP. For example, the rate of photoinduced electron transfer from TiO_2 NPs to Au nanoclusters increases by two orders of magnitude as the composition of gold NPs changes from Au_{38} to Au_{4033}.

In the systems with the ohmic contact between the semiconductor and metal NPs, for example, TiO_2/Pt or ZnO/Pt, the size-dependent increment of the capacity of metal NPs is accompanied by the enhancement of electron-hole recombination and the decrease of the rate of competing photocatalytic reactions.

Growth of the metal NP size in the nanostructures with non-ohmic (Schottky) semiconductor–metal contact, for example, TiO_2/Au, TiO_2/Ag , ZnO/Au, ZnO/Ag results in lowering of the collective Fermi level and gradual disappearing of the photocatalytic properties. Mesoporous and 3D-organized semiconductor nanophotocatalysts have higher surface energy and reduced surface tension. It needs less agglomeration and arrest growth of semiconductor crystals on the phase of NP formation. The mesoporous materials show (i) a developed surface area (100-300 m^2/g) and the nanometer pore size favoring to substrates adsorption on the inner pore surface till the capillary condensation; (ii) a prolonged time of the substrate retention in the mesopores allowing protracted contact between the semiconductor NPs and a substrate; (iii) migration of the photogenerated charge carriers among the adjoining semiconductor NPs and their accumulation in the points of NPs contact; and, finally, (iv) in case of mesoporous hollow micro-spheres. Mesoporous semiconductor materials show much higher photocatalytic activity than corresponding non-porous materials.

The mesoporous Cu_2O, CeO_2, and V_2O_5 show higher photocatalytic activity. Semiconductor NPs – nanorods, nano-sheets, nanowires, etc., reveal higher photocatalytic properties as compared with the spherical- or faceted-shaped NPs of the same composition because of photogenerated electrons travel along the nanosheet and reduce the metals on the nanosheet edges. For example, MnO_2 NPs are deposited on the surface of nanosheets as a results of Mn^{II} oxidation by the valence band holes indicating random hole movement. The rutile TiO_2 nanorods show higher photocatalytic activity in phenol oxidation as compared with the spherical titania NPs. The ordered nanocrystalline TiO_2 films formed by the nanorods, oriented perpendicular to the substrate, are more efficient photocatalysts of water splitting than the conventional TiO_2 films formed by fractal aggregates of TiO_2 NPs.

The nanocrystalline semiconductor nanocrystalline TiO_2 electrodes involves coating of a conductive glass plate with paste containing TiO_2 NPs mixed with waxy agents followed by the calcination at 350-400 °C. The photoctalysis in nanocrystalline titania is usable in oxidation of dyes, glucose, sodium benzylsulfonate and dodecylsulfonate; mineralization of formic, oxalic, and succinic acid, some aminoacids, and 4-chlorophenol; vapor-phase oxidation of formaldehyde; disruption of the cell membranes of bacteria, and hydrogen evolution from water-alcohol solutions.

The porous films of nanocrystalline WO_3 and TiO_2 nanotube arrays show the photoelectrocatalytic activity toward pentachlorophenol oxidation. The nanocrystalline Nb_6O_{17}, $Ca_2Nb_3O_{10}$, $Ti_{0.91}O_2$, Ti_4O_9, and MnO_2 electrodes have the photoelectrocatalytic properties in methanol oxidation. The nanocrystalline Bi_2MoO_6 films are photoelectrocatalytically active in dyes destruction.

The photoelectrocatalytic activity in water splitting and water reduction at the expense of sacrificial donors was observed for the nanotubes of titania and alkali metal titanates, nanocrystalline films of TiO_2, TiO_2/Au, WO_3, Cu_2O, and TiO_2 nanowire arrays. High efficiency of light-to-current conversion was observed for the nanocrystalline electrodes composed of nitrogen-, boron-, silicon- , carbon-doped titanate nanotubes, the films of TiO_2 hollow microspheres, dye-sensitized nanocrystalline films of TiO_2, Nb_2O_5, $SrTiO_3$, ZnO, and α-Fe_2O_3, the self-assembled films of titania nanosheets, ZnO/TiO_2, NiO, Bi_2S_3, CdS and CdS/Au, and β-In_2S_3

4 CONCLUSION

The photocatalytic action of a semiconductor crystal,arises from the photogeneration of electrons and holes. Nanosemiconductor crystals show quantum size effects. Nanophotocatalysis is useful in a design of coupled semiconductor nanostructures, photoinduced polarization of semiconductor NPs, photopolarization effect in the nanocrystalline semiconductors. Now optical and electronic and photocatalytic photophysical and photoexcitation of semiconductor crystals, and quantum phenomena is new excitement in the ultra-small semiconductor particle.